



Thermal and Exergy Assessment of a Micro Combustor Fueled by Premixed Hydrogen/Air under Different Sizes: a Numerical Simulation

E. Nadimi[†] and S. Jafarmadar

Department of Mechanical Engineering, School of Engineering, Urmia University, Urmia, West Azerbaijan, Iran

[†]Corresponding Author Email: st_e.nadimi@urmia.ac.ir

(Received October 18, 2019; accepted December 31, 2019)

ABSTRACT

In this work, a numerical study has been carried out in order to investigate the effects of a micro combustor size on the exergy and energy efficiencies of a premixed hydrogen/air for a micro thermophotovoltaic system. For this purpose, six combustors in different sizes are designed, in which geometry dimensional size gradually reduced. The effects of the combustor size on the entropy, exergy, radiation power, and energy conversion efficiency are investigated. Also, mean and uniform wall temperature are discussed. In order to compare the entropy generation of each micro combustor, a dimensionless entropy generation rate is defined. The hydrogen/air combustion with 9 species and 19 reversible elementary reactions were simulated by using the Eddy Dissipation Concept (EDC) model. Results indicate the micro-combustor geometry size has important effects. A reduction of the combustor geometry size dimensionality causes an increase in average wall temperature and makes it uniform. Moreover, by decreasing micro combustor size, the radiation power efficiency increases from 41.96 to 45.62% and total energy conversion efficiency from 6.46 to 7.02%. The highest exergy efficiency, 38.63%, is achieved in the smallest micro combustor while the minimum exergy efficiency 33.22%, is obtained in the largest micro combustor.

Keywords: Micro combustor size; Wall temperature; Entropy generation; Exergy efficiency; Thermal performance.

NOMENCLATURE

A_i	The surface area of element i on the external wall	L_1	Micro combustor length
$C_{p_{outlet}}$	Specific heat capacity of the exhaust gases	L_2	Micro combustor step length
D_1	The inlet diameter	\dot{m}	Inlet mass flow rate
D_2	The outlet diameter	\dot{m}_{H_2}	Hydrogen mass flow rate
D_3	The outer diameter of the micro combustor	n_j	The number density of species j
\dot{E}_{loss}	The energy loss	P_0	Ambient pressure
E_T	Total fluid energy	\dot{Q}_R	Chemical heat release rate
$\dot{E}_{x_{loss}}$	Exergy loss	\dot{Q}_{Rad}	Radiation heat transfer
h_0	Free convection heat transfer coefficient	\dot{Q}_{wall}	Heat transfer from the external wall
h_j	Enthalpy of each species	R_{outlet}	Specific gas constant at the outlet
I	Unit tensor	R_u	Ideal gas constant
\vec{J}_j	Diffusion flux of species j	R_T	Nonuniformity coefficient
k_f	Fluid conductivity	S_f	Enthalpy source
K_s	Solid zone thermal conductivity	s	Specific entropy
		\dot{S}_{gen}	Total entropy generation rate

T_i	The temperature of element i	ω_j	Reaction rate
T_m	Mean wall temperature	η_{II}	Exergy efficiency
T_{outlet}	Outlet Temperature	σ	Boltzmann constant
\vec{u}	Velocity vector	ε	Surface emissivity
u	Specific internal energy	Abbreviations	
\bar{w}	Average molecular weight	con	Conversion
Y_j	Mass fraction of each species	gen	Generation
ρ	Density	in	Inlet
μ	Molecular viscosity	LHV	Low heat value
μ_j	Chemical potential of each species	rad	Radiation
		sur	Surrounding
		TPV	Thermophotovoltaic

1. INTRODUCTION

Today, small-scale devices are being developed, with the appearance of science and technology, and need to construct small-scale devices. Energy sources for these devices are batteries, micro gas turbines, micro thermophotovoltaic systems. Batteries have limitations such as a low energy density, long recharging time, relatively short lifetime, heavyweight. The Micro Thermophotovoltaic (MTPV) power generator is one of the best choices for power generation because it has not included any moving parts, easy to manufacture, and high energy density (Su *et al.* (2015)). The MTPV systems include three basic parts, which are a combustion chamber, a PV cell array, and an emitter (Yang *et al.* (2002)). To illustrate the function of the MTPV systems, chemical energy during a combustion process of hydrogen and air causes rising the wall temperature of a micro combustor and thermal radiation flux released from the combustor wall. It is absorbed by the PV cell array, and then electric power is generated.

A lot of researches have been done to improve radiation heat transfer, energy efficiency, flame stability, uniform wall temperature, and structure optimization for a micro combustor of the MTPV system. Yang *et al.* (2007) experimentally studied micro cylindrical combustor with a backward-facing step and the combustor diameter. They show that raising the height of the backward-facing step of the micro combustor and reducing the combustor diameter can improve the short circuit current total energy conversion of the MTPV device. Wan *et al.* (2012) investigated experimentally and numerically lean hydrogen-air combustion in a planar micro combustor with a bluff body and found that increasing the equivalence ratio from 0.4 to 0.6 causes an increase in the blow-off limit range. Moreover, with increasing inlet velocity, the flame is long and becomes thin, and the high-temperature zone of wall shifts downstream. A uniform and high wall temperature distribution on the micro combustor is effective to receive higher energy efficiency. Gradually reducing the wall thickness of the micro-cylindrical combustor makes wall

temperature distribution higher and more uniform, which is proposed by Zuo *et al.* (2017). Akhtar *et al.* (2015) showed the effects of channel cross-section (circular, rectangular, square, trapezoidal, and triangular) on the total efficiency. Also, they reported that a Reynolds Stress Model (RSM) for turbulent flow with the Eddy Dissipation Concept (EDC) model for combustion processes, gives the best prediction of the wall temperature. Su *et al.* (2015) found that the usage of a two-cavity and one-cavity for the micro combustor caused that radiation power is increased from 2.1 W for one cavity to 2.5 W for two cavities. The irreversible energy loss and entropy generation in combustion processes cannot be neglected. The entropy generation in the micro-combustion process has been carried out by some researchers (Peng *et al.* (2018); Huang *et al.* (2019)). In recent years, exergy analysis has been used for the micro combustor. Jiaqiang *et al.* (2016) investigated the effect of inlet pressure on entropy generation and temperature distribution in premixed hydrogen-air combustion in a circular micro-combustor. Their results suggested that when inlet pressure is $P = 100$ KPa, the maximum exergy efficiency is reached 40 percent. The minimum exergy efficiency is obtained 36 percent when the inlet pressure is $P = 60$ KPa. Moreover, they reported that the maximum average wall temperature is achieved at $P = 0$ KPa while the highest wall temperature difference is reported at $P = 100$ KPa. Also, the maximum energy efficiency is obtained at $P = 20$ KPa. The bluff body was used to improve uniform wall temperature and micro combustor performance. Jiang *et al.* (2014) numerically studied the entropy generation distribution in the hydrogen-air mixer in the micro combustor. Their numerical results showed that the stoichiometric mixture has maximum entropy generation but minimum entropy generation is obtained in a rich and lean premixed hydrogen-air. Ni *et al.* (2019) numerically studied a micro combustor with the rib, they observed that the micro combustor with two ribs works more efficiently than one rib. they reported that the chemical reaction contributed about 70 percent of the total entropy generation.

Many types of research have been done on micro

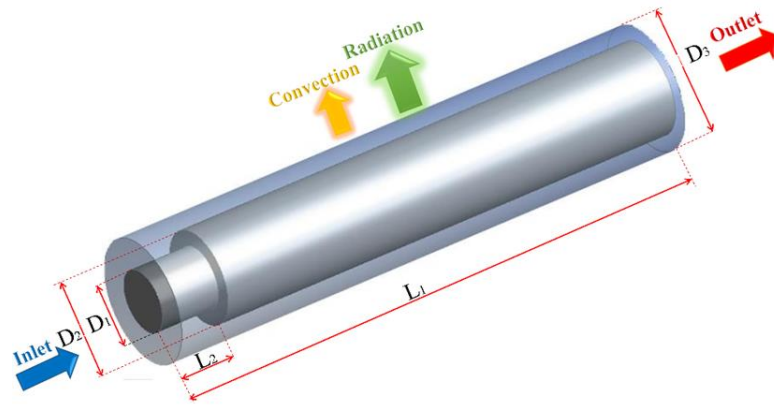


Fig. 1. Schematic of the micro-combustor.

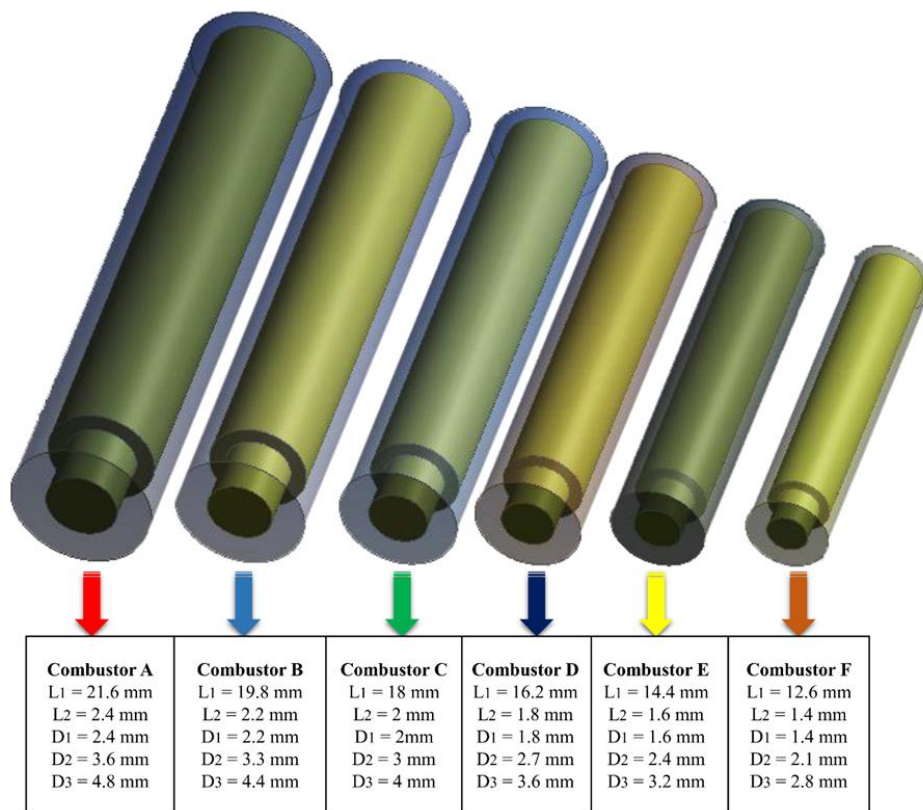


Fig. 2. Geometry and dimensions of the micro combustors.

combustor, but most of them have been studied to achieve uniform wall temperature and to increase the energy performance and electric power production of the MTPV systems. No research has so far been carried out to study the effect of the micro-combustor size on the entropy generation distribution, total energy efficiency, and exergy efficiency. In this work, a three-dimensional simulation and numerical investigation of the effects of the micro-combustor scale on the entropy generation, exergy efficiency and wall temperature have been done under the same boundary conditions where inlet velocity is 5 m/s, and the premixed

H_2 /air equivalence is 1.

2. DESCRIPTION OF THE NUMERICAL MODEL

2.1. Micro Combustor Geometry

The micro-combustor geometry is shown in Fig. 1. The total length (L_1); step length (L_2); inlet diameter (D_1); outlet diameter (D_2), and the outer diameter (D_3) are the dimensions of the micro-combustors. The micro combustors are made of 316 stainless steel, which its physical properties presented in

Table 1 (Wan *et al.* (2015)). We used six micro combustors (A, B, C, D, E, F) in different scales for CFD simulation. Its sizes can be seen in Fig. 2.

Properties	Density	Thermal conductivity	Specific heat
stainless steel	8000	12.0	503

2.2. Mathematical Model

Before building the pursuant governing equations, some assumptions are essential for simplifying the mathematical model as follows: (a) combustion process is a steady-state; (b) The H₂/air premixed is uniform; (c) No Dufour effect (Williams (1965)); (d) The work done by pressure forces and viscous are ignored; (e) No gas radiation in the combustion channel but the radiation between the out wall and the environment are considered (Norton *et al.* (2004)); (f) No surface reactions.

The governing equations are then given as follows:

Continuity and momentum conservation equation:

$$\nabla \cdot (\rho \vec{u}) = 0 \tag{1}$$

$$\rho(\vec{u} \cdot \nabla \vec{u}) = -\nabla P + \nabla \cdot \left[(\mu + \mu_T) \left[\nabla \vec{u} + (\nabla \vec{u})^T - \frac{2}{3} \nabla \cdot \vec{u} I \right] \right] \tag{2}$$

Where ρ and \vec{u} are the fluid density and the velocity vector. And P is the pressure, μ_T is the turbulent viscosity, and I is the unit tensor.

Energy conservation equation:

$$\nabla \cdot \vec{u} (\rho E_T + P) = \nabla \cdot \left[\left(k_f + \frac{C_p \mu_T}{Pr_T} \right) \nabla T - \left(\sum_j h_j \vec{J}_j \right) \right] + \nabla \cdot \left[(\mu + \mu_T) \left(\nabla \vec{u} + (\nabla \vec{u})^T - \frac{2}{3} \nabla \cdot \vec{u} I \right) \right] \cdot \vec{u} + S_f \tag{3}$$

Where E_T is total fluid energy, k_f is the fluid conductivity, Pr_T is the turbulent Prandtl number, \vec{J}_j is the diffusion flux of species j , h_j is the enthalpy of species j , and S_f is the fluid enthalpy source.

Energy equation for the solid zone:

$$\nabla \cdot (K_s \cdot \nabla T) = 0 \tag{4}$$

Where K_s denotes the solid domain thermal conductivity

*Ideal gas equation (Alipoor *et al.* (2017)):*

$$P = \rho \frac{R_u}{\bar{W}} T \tag{5}$$

Where \bar{W} and R_u are the average of molecular weight of the H₂/air mixture and the ideal gas

constant.

Species transport equations:

$$\nabla \cdot (\rho \vec{u} Y_j) = \nabla \cdot \vec{J}_j + \omega_j \tag{6}$$

Where ω_j is the net production rate of species j .

Entropy transport equation:

$$T ds = du + Pd \left(\frac{1}{\rho} \right) - \sum_{j=1}^n \mu_j d \left(\frac{n_j}{\rho} \right) \tag{7}$$

$$\dot{S}_{gen} = \dot{m} (s_{outlet} - s_{in}) \tag{8}$$

Where \dot{S}_{gen} is the total entropy generation rate, s is the specific entropy, \dot{m} is the mass flow rate, u and μ_j are the internal energy and the chemical potential of each species, and n_j is the number density of species j .

Under the second law of thermodynamics, exergy loss, and the exergy efficiency (Sahoo *et al.* (2012)) are defining as below:

$$\dot{E}x_{in} = \dot{m}_{H_2} \times Q_{LHV} \tag{9}$$

$$\dot{E}x_{loss} = \dot{E}x_{loss} + \left[\dot{m} \times T_{sur} \times \left(C_{p_{outlet}} \ln \frac{T_{sur}}{T_{outlet}} - R_{outlet} \ln \frac{P_0}{P_{outlet}} \right) \right] \tag{10}$$

$$\eta_{II} = \frac{\dot{E}x_{in} - \dot{E}x_{loss}}{\dot{E}x_{in}} \tag{11}$$

Where $\dot{E}x_{loss}$ is the energy loss by the outlet gases, Q_{LHV} is hydrogen lower heating value that is assumed to be 119 MJ/kg (Turns (2002)).

The total heat transfer (\dot{Q}_{wall}) between the external wall of the micro combustor and the environment is defined as follows:

$$\dot{Q}_{wall} = \dot{Q}_{Rad} + \dot{Q}_{con} \tag{12}$$

$$\dot{Q}_{Rad} = \varepsilon \sigma \sum_{i=1}^n A_i (T_i^4 - T_{sur}^4) \tag{13}$$

$$\dot{Q}_{Con} = h_0 (T_i - T_{sur}) \tag{14}$$

Where σ , ε are Boltzmann constant and surface emissivity, respectively. T_i , A_i are the temperature and the surface area of element i at the outer wall and h_0 is the heat transfer coefficient.

The radiation power efficiency (η_{Rad}) is defined as the ratio of the radiation heat transfer rate (\dot{Q}_{Rad}) from the outer wall of the micro-combustor to the heat of reaction (\dot{Q}_R):

$$\eta_{Rad} = \frac{\dot{Q}_{Rad}}{\dot{Q}_R} \tag{15}$$

The total energy conversion efficiency in the micro

Table 2 H₂/air chemical reaction mechanism

Reaction	A (m ³ /kmol s)	β	E (J/kmol)
H + O ₂ = O + OH	5.1×10 ¹³	-0.82	6.91×10 ⁷
H ₂ + O = H + OH	1.8×10 ⁷	1.0	3.7×10 ⁷
H ₂ + OH = H ₂ O + H	1.2×10 ⁷	1.3	1.52×10 ⁷
OH + OH = H ₂ O + O	6.0×10 ⁶	1.3	0.0
H + OH + M = H ₂ O + M ^a	7.5×10 ¹⁷	-2.6	0.0
O ₂ + M = O + O + M	1.9×10 ⁸	0.5	4.001×10 ⁸
H ₂ + M = H + H + M ^b	2.2×10 ⁹	0.5	3.877×10 ⁸
H ₂ + O ₂ = OH + OH	1.7×10 ⁸	0.0	2.0×10 ⁸
H + O ₂ + M = HO ₂ + M ^c	2.1×10 ¹²	-1.0	0.0
H + O ₂ + O ₂ = HO ₂ + O ₂	6.7×10 ¹³	-1.42	0.0
H + O ₂ + N ₂ = HO ₂ + N ₂	6.7×10 ¹³	-1.42	0.0
HO ₂ + H = H ₂ + O ₂	2.5×10 ¹⁰	0.0	2.9×10 ⁶
HO ₂ + H = OH + OH	2.5×10 ¹¹	0.0	7.9×10 ⁶
HO ₂ + O = OH + O ₂	4.8×10 ¹⁰	0.0	4.2×10 ⁶
HO ₂ + OH = H ₂ O + O ₂	5.0×10 ¹⁰	0.0	4.2×10 ⁶
HO ₂ + HO ₂ = H ₂ O ₂ + O ₂	2.0×10 ¹⁰	0.0	0.0
H ₂ O ₂ + M = OH + OH + M	1.3×10 ¹⁴	0.0	1.905×10 ⁸
H ₂ O ₂ + H = HO ₂ + H ₂	1.7×10 ⁹	0.0	1.57×10 ⁷
H ₂ O ₂ + OH = H ₂ O + HO ₂	1.0×10 ¹⁰	0.0	7.5×10 ⁶

^a Enhancement factors: H₂O/20/.
^b Enhancement factors: H₂O/6/, H/2/, H₂/3/.
^c Enhancement factors: H₂O/21/, H₂/3.3/, O₂/0/, N₂/0/.

Table 3 Boundary conditions

Boundary	Parameters	Values
Inlet	Velocity inlet	5 m/s
	Gage pressure	0 Pa
	Turbulent intensity	5 %
	The hydraulic diameter	Regard to inlet diameter
	Temperature	300 K
Outlet	Gage outlet pressure	0 Pa
	Turbulent intensity	5 %
	The hydraulic diameter	Regard to outlet diameter
Inner wall	Interface No-slip	zero-flux for all species
	Thermal condition	coupled
	Material	steel
Out wall	Radiation and convection	Mixed
	Heat transfer coefficient	15 W/m ² K
	Emissivity	0.7

combustor for MTPV systems is defined as:

$$\eta_{\text{tot}} = \eta_{\text{TPV}} \cdot \eta_{\text{Rad}} \quad (16)$$

where η_{TPV} is MTPV systems efficiency that is assumed to be 15.4% (Xue *et al.* (2005)).

Two parameters to measure the nonuniformity coefficient of outer wall temperature (R_T) and mean

outer wall temperature (T_m) are defined as below (Ansari *et al.* (2018)):

$$R_T = \left(\frac{\sum_{i=1}^n [T_i - T_m] A_i}{T_m \sum_{i=1}^n A_i} \right) \times 100 \quad (17)$$

$$T_m = \frac{\sum_{i=1}^n T_i A_i}{\sum_{i=1}^n A_i} \quad (18)$$

2.3. Numerical Setup

For the numerical simulation, the Ansys Fluent 17 has been used to solve the governing equations. The coupled algorithm is applied for the velocity pressure decoupling of the Navier-Stokes equations (Jiang *et al.* 2015). The standard k-ε model (Kuo *et al.* (2007)) is used for turbulent flow and the eddy dissipation concept (EDC) model (Akhtar *et al.* (2015)) are applied for the chemical reaction. 9 species and 19 reversible reaction mechanisms of H₂/air are given in Table 2 (Yang *et al.* (2014)). The specific heat and the density of the premixed hydrogen-air mixture are computed by incompressible ideal gas law and mixing law, respectively. Viscosity and gas thermal conductivities of the mixture are computed by the weighted mass fraction of all species, and the specific heat of each species is computed utilizing a sectioned polynomial method (Tang *et al.* (2015a, b)), kinetic theory is used to calculate the mass diffusivity of the H₂/air mixture. The convergence criterion of continuity, momentum, and species equations are 1×10⁻⁴, and lower than 1×10⁻⁶ for the energy equation.

Besides, the boundary conditions in the current work are shown in Table 3.

2.4. Grid Independency

In order to determine the minimum number of grid cells to guarantee that the present numerical simulation is independent of the grid cells, moreover, to reduce the computational time, the grid sensitivity is tested (Fig. 3). Three meshes (517610, 759278, and 913851) are used to study the wall temperature profile of combustor C, where premixed hydrogen-air velocity is kept at 5 m/s. As presented in Fig. 4, the difference in the wall temperature distribution on the three meshes is very small and over 913851 elements, the wall temperature wasn't changed. So, the mesh structure about 913851 cells is used for an accurate simulation.

2.5. Validation of the numerical simulation

To validate the numerical simulation of this study, the temperature distribution of the micro-combustor wall is compared with the experimental data reported by Wenming *et al.* (2015) and with our previous work (Nadimi *et al.* (2019)). As presented in Fig. 5, in this work, we used dimensionless length, which is defined as z axial per the total length of the micro-combustor (z/L). We considered wall temperature of the micro combustor C where H₂/air equivalence ratio and the inlet velocity are 1 and 5 m/s, respectively. As shown in this figure, there is a discrepancy at first between experimental results and numerical simulation. However, the

maximum difference in the two temperature profiles is 6% at the beginning of the micro combustor. But this difference is reduced throughout the length of the micro combustor. This error is due to the rectangular cross-section for the micro combustor in experimental results. But in this research, the circular cross-section has been used. Akhtar *et al.* (2015) discussed the reasons for this difference. However, this simulation is in good agreement with our previous work.

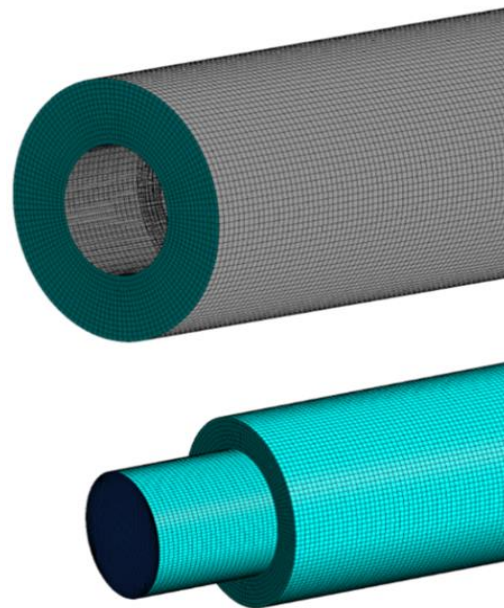


Fig. 3. The computational grid for solid and reaction zones.

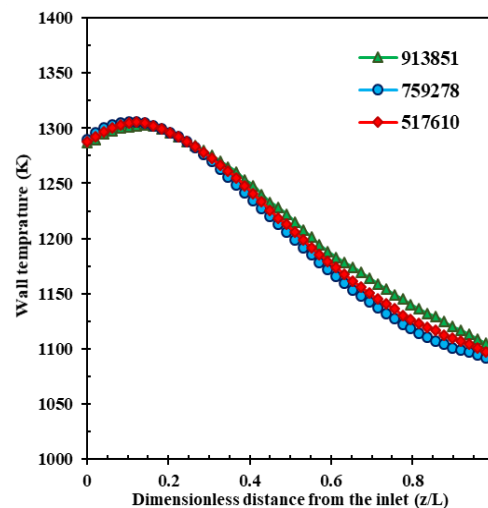


Fig. 4. Mesh independence study for combustor C.

3. RESULTS AND DISCUSSIONS

3.1. Effects of Micro Combustor Size on Entropy

Figure 6 presents the entropy generation under various micro combustor size. It can be observed that the variety of micro combustor sizes have essential effects on the entropy generation. By increasing the size of the micro-combustor, the mass flow rate of the inlet increases. It causes an increase in the total entropy generation rate. Figure 7 shows the specific entropy distribution for three micro combustors. It is observed in Fig. 7 that the specific entropy of the smallest micro combustor is lower than that of the largest micro combustor under the same condition. The high entropy areas of them are located in the central region of the micro combustors (contour lines 20, 19, and 18). These high entropy areas are gotten smaller by decreasing the size of micro combustors. The micro combustor F causes a lower specific entropy region, that is the major reason why the total entropy generation of the smallest micro combustor is lower than that of others.

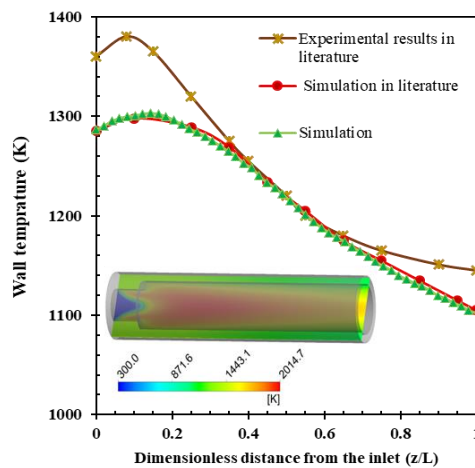


Fig. 5. Validation of the numerical results with experimental data and numerical simulation in literature.

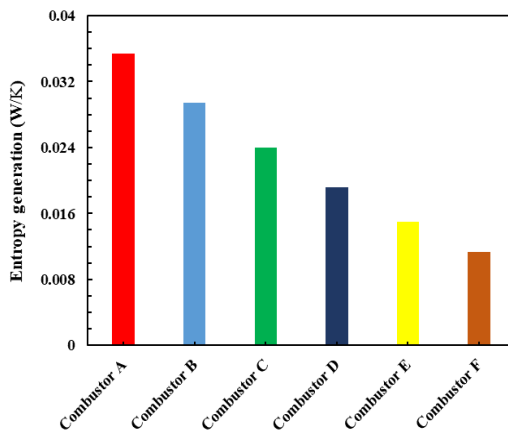


Fig. 6. Entropy generation rate under different micro combustors.

To determine the relationship between the size of the micro combustors and entropy generation rate,

we need to normalize the rate of entropy generation and the volume of the micro combustors. To do this, we use the volume and entropy generation rate of micro combustor C, $S_{Dim} = \dot{S}_{gen} / \dot{S}_{gen_C}$, $V_{Dim} = V / V_C$. As it is observed in Fig. 8 with the increasing value of the dimensionless volume, the dimensionless entropy generation rate is increasing due to the high mass flow rate.

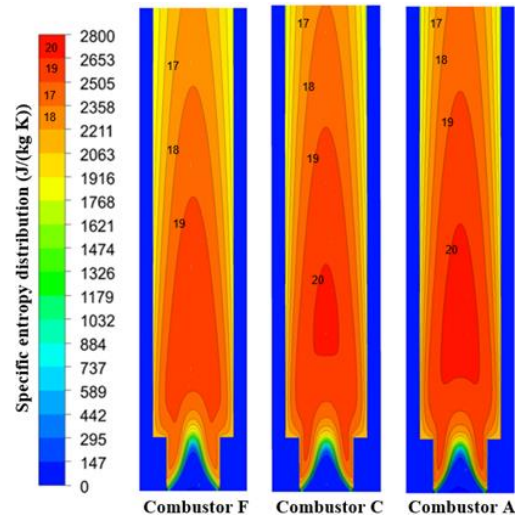


Fig. 7. Effects of micro combustor sizes on specific entropy of premixed hydrogen-air.

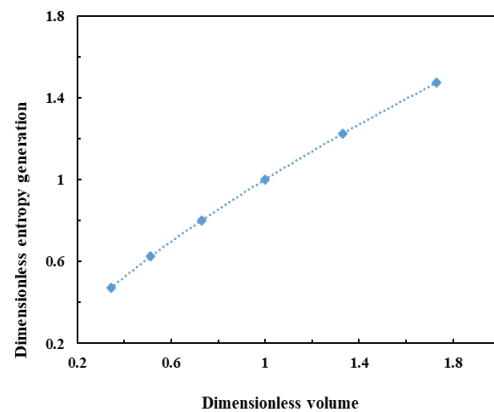
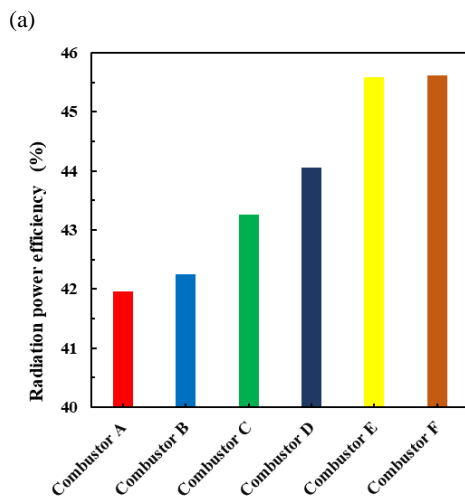
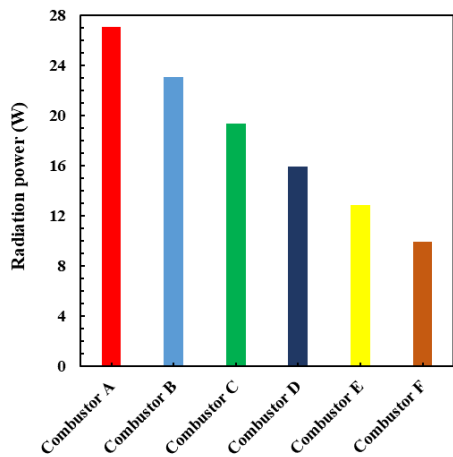


Fig. 8. Dimensionless entropy generation under dimensionless volume.

3.2. Effects of Micro Combustor Size on Radiation

Figure 9(a) depicts the radiation power and radiation power efficiency of the micro combustors at a different size. Radiation power has an inverse correlate with micro combustor size. The highest radiation power is obtained by the biggest micro combustor. So, the micro combustor A has a maximum radiation power, and micro combustor F has a minimum. While micro combustor F has a high mean wall temperature. That's due to the radiation power, according to Eq. 13 has a direct relationship with the out wall surface area. Based on Eq. 15, the radiation power efficiency has defined the ratio of the radiation power through the micro-

combustor wall to the total energy input. Therefore, with the increase in the size of the combustor, the total input energy increased, so radiation power efficiency reduces, as shown in Fig. 9(b). The micro combustor F has a maximum radiation power efficiency, whereas this only 0.04 percent point is higher than micro combustor E. The difference between micro combustor A and B is 1.52 percent point. The difference between the largest and smallest micro combustor radiation power efficiency (A, F) is only a 3.66 percent point. While the radiation power is decreased almost three times from 64.45W to 21.83W. This radiation power can generate 4.1 W to 1.5 W of electricity. This means that radiation power efficiency does not change more compared with the radiation power by decreasing the size of the micro combustor smaller.



(a) (b)
Fig. 9. (a) Radiation power rate and (b) radiation power efficiency under different micro combustors.

3.3. Effects of Micro Combustor Size on Temperature

In order to investigate the effects of micro combustor size on the temperature field, the mean outer wall temperature, nonuniformity coefficient, and contour of temperature at outlet regions are

presented in Fig. 10 and Fig. 11, respectively. As shown in Fig. 10 by decreasing the micro combustor size, the mean wall temperature faces an increase from 1195.7 K to 1221.6 K, and the non-uniformity coefficient is decreasing from 6.04 to 5.29 and the least amount of non-uniformity coefficient indicates more uniform wall temperature. When the dimensions of combustor are reduced by 1.71 times, the mean out wall temperature increased 25.85K, and the nonuniformity coefficient is decreasing by 12.35%. Figure 11 shows the contours of outlet temperature at different micro combustors. To compare the contours of outlet temperature, we have changed the contours to the same size. For all contours, the outlet temperature climbs up to the peak when moving from an inner wall to a center of the micro combustors. A high-temperature region at the outlet is decreased by making the size of the micro-combustor smaller. The high-temperature distribution at the outlet surface causes that the energy brought away by the outlet gases are increasing.

3.4. Effects of Micro Combustor size on Exergy Efficiency

As the size of the micro-combustor reduces, the entropy generation and the temperature of the exhaust gases decrease. Therefore, the exergy loss is diminished, according to Eq. 10, as depicted in Fig. 12(a). The exergy loss is reduced to a considerable level by reducing the micro combustor size. it is decreased from 43.04 W to 13.39 W for the largest to the smallest micro combustor.

Based on the above results and Eq. 11, Fig. 12(b) depicts the exergy efficiency for each combustor. The highest exergy efficiency 38.63% achieved in the combustor F but, minimum exergy efficiency 33.22% obtained in the combustor A. When the dimension of the combustor A is reduced to the combustor F (1.71 times reduction), the exergy efficiency is increased by 5.41 percent point, and the exergy loss is decreased by 68.88%.

To summarize, Table 4 represents various parameters to study the MTPV systems. The signs ↓ and ↑ indicate reduce and increase of the parameters. To select the best micro combustor in terms of mean wall temperature (T_m), radiation power efficiency (η_{Rad}), exergy efficiency (η_{II}), and total energy conversion efficiency (η_{tot}). The micro combustor F has the maximum total energy conversion efficiency (7.02%), and it is suitable for MTPV systems.

4. CONCLUSIONS

In the present work, a 3D simulation and numerical investigation of the effects of the micro-combustor geometry size gradually reducing on entropy generation, exergy efficiency, and radiation power efficiency have been studied. For this purpose, six micro combustor geometries were constructed

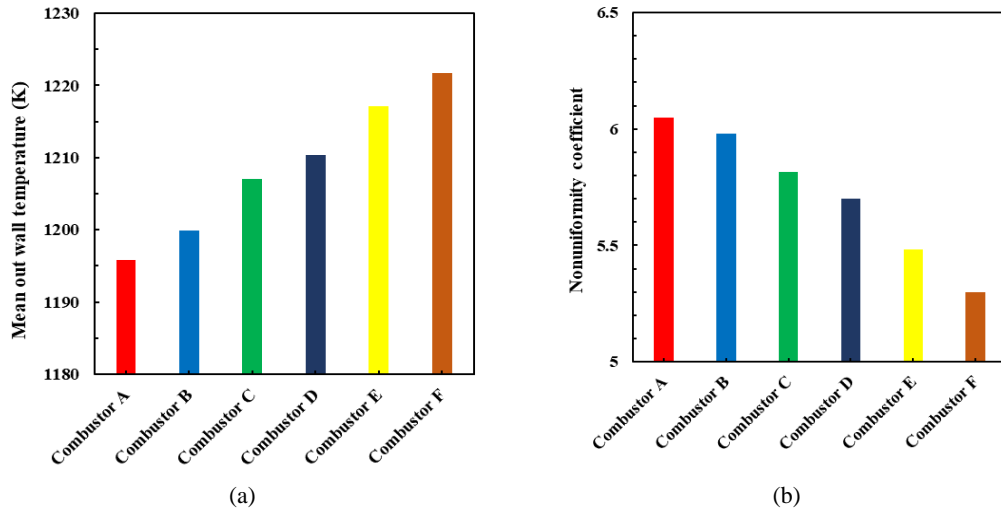


Fig. 10. (a) Mean out wall temperature and (b) nonuniformity coefficient under different micro combustors.

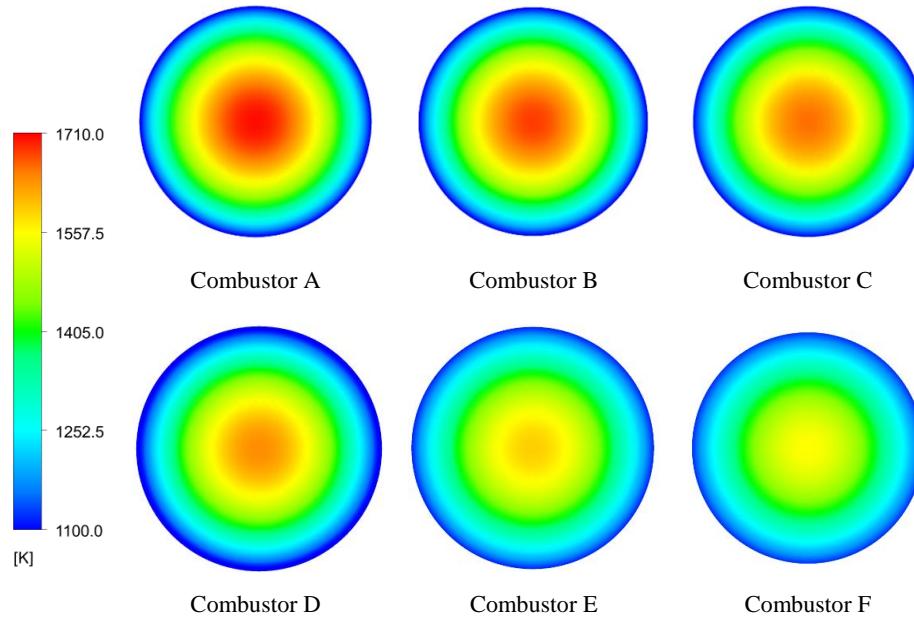


Fig. 11. Contours of outlet temperature for different micro combustors.

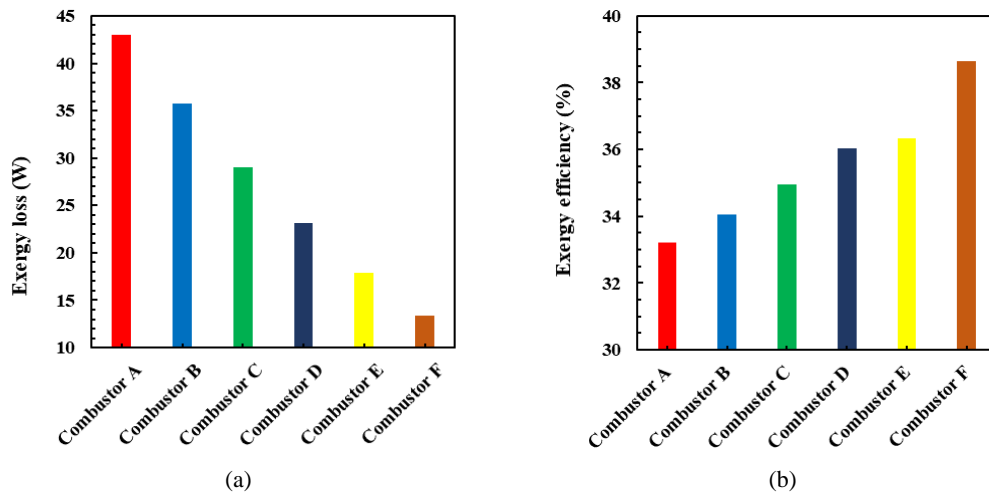


Fig. 12. (a) Exergy loss and (b) exergy efficiency for different micro combustors.

Table 4 various parameters on the micro combustor performance for MTPV systems. The signs ↓ and ↑ indicate the reduction and increase of the parameters

Parameters	\dot{Q}_R	\dot{Q}_{wall}	\dot{Q}_{Rad}	\dot{S}_{gen}	$\dot{E}x_{loss}$	T_m	R_T	η_{Rad}	η_{II}	η_{tot}
Combustor A	64.45	31.47	27.05	0.035	43.04	1195.7	6.04	41.96	33.22	6.46
Combustor B	54.15	26.72	23.03	0.029	35.70	1199.9	5.98	42.25	34.06	6.50
Combustor C	44.68	22.39	19.33	0.024	29.06	1207.0	5.81	43.26	34.95	6.66
Combustor D	36.13	18.41	15.92	0.019	23.10	1210.3	5.69	44.06	36.04	6.78
Combustor E	28.16	13.43	12.84	0.015	17.93	1217.1	5.48	45.58	36.34	7.01
Combustor F	21.83	11.49	9.963	0.013	13.39	1221.6	5.29	45.62	38.63	7.02
Decreasing combustor size	↓	↓	↓	↓	↓	↑	↓	↑	↑	↑

under the same boundary conditions for micro TPV systems. The main results of the present work are concluded as follows:

- The micro combustor size has important effects on the temperature, entropy generation, exergy, and radiation of the micro combustors.
- By decreasing micro combustor size, the radiation power decreases but, radiation power efficiency increases. The micro-combustor F has a maximum radiation power efficiency 45.62%, while it has minimum radiation power 9.96W.
- The highest mean wall temperature 1221.64 K, and the least nonuniformity coefficient 5.29 obtain at the smallest micro combustor (micro combustor F).
- When the size of the combustor A 1.71 times reduce, exergy loss decreases to 29.64 W, and entropy generation decreases by 68%.
- The highest exergy efficiency 38.63% achieved in the combustor F but the minimum exergy efficiency 33.22% obtained in the combustor A. For the same micro combustor geometry and boundary conditions, by decreasing the micro-combustor geometry size performance of the micro-combustor improved from the perspective of the second law of thermodynamics.

CONFLICT OF INTERESTS

The authors declare that they have no conflict of interests regarding the publication of this paper.

REFERENCES

Akhtar, S., J. C. Kurnia and T. Shamim (2015) A three-dimensional computational model of H₂-air premixed combustion in non-circular micro-channels for a thermo-photovoltaic (TPV) application. *Applied Energy* 152, 47-57.

Alipoor, A. and M. H. Saidi (2017 Aug). Numerical study of hydrogen-air combustion characteristics in a novel micro-thermophotovoltaic power generator. *Applied Energy* 199, 382-399.

Ansari, M. and E. Amani (2018). Micro-combustor

performance enhancement using a novel combined baffle-bluff configuration. *Chemical Engineering Science* 175, 243-56.

Huang, Q., A. Tang, T. Cai, D. Zhao and C. Zhou (2019). Entropy generation analysis of combustion process adopting blended propane/hydrogen fuels in micro-combustor. *Chemical Engineering and Processing-Process Intensification* 143, 107601.

Jiang, D., W. Yang and J. Teng (2015). Entropy generation analysis of fuel lean premixed CO/H₂/air flames. *International Journal of Hydrogen Energy* 40 (15), 5210-20.

Jiang, D., W. Yang, K. J. Chua, J. Ouyang and J. H. Teng (2014). Analysis of entropy generation distribution in micro-combustors with baffles. *International Journal of Hydrogen Energy* 39(15), 8118-25.

Jiaqiang, E., W. Zuo, X. Liu, Q. Peng, Y. Deng and H. Zhu (2016). Effects of inlet pressure on wall temperature and exergy efficiency of the micro-cylindrical combustor with a step. *Applied Energy* 175, 337-45.

Kuo, C. H. and P. D. Ronney (2007) Numerical modeling of non-adiabatic heat-recirculating combustors. *Proceedings of the Combustion Institute* 31(2), 3277-84.

Nadimi, E. and S. Jafarmadar (2019). The numerical study of the energy and exergy efficiencies of the micro-combustor by the internal micro-fin for thermophotovoltaic systems. *Journal of Cleaner Production* 235, 394-403.

Ni, S., D. Zhao, Y. Sun and E. Jiaqiang (2019). Numerical and entropy studies of hydrogen-fuelled micro-combustors with different geometric shaped ribs. *International Journal of Hydrogen Energy* 44(14),7692-705.

Norton, D. G. and D. G. Vlachos (2004). A CFD study of propane/air microflame stability. *Combustion and Flame* 138(1-2), 97-107.

Peng, Q., E. Jiaqiang, Z. Zhang, W. Hu, X. Zhao (2018). Investigation on the effects of front-cavity on flame location and thermal performance of a cylindrical micro combustor. *Applied Thermal Engineering* 130, 541-51.

- Sahoo, B. B., U. K. Saha and N. Sahoo (2012). Diagnosing the effects of pilot fuel quality on exergy terms in a biogas run dual fuel diesel engine. *International Journal of Exergy* 10(1),77-93.
- Su, Y., J. Song, J. Chai, Q. Cheng, Z. Luo, C. Lou and P. Fu (2015). Numerical investigation of a novel micro combustor with double-cavity for micro-thermophotovoltaic system. *Energy Conversion and Management* 106,173-80.
- Tang, A., J. Pan, W. Yang, Y. Xu and Z. Hou (2015a). Numerical study of premixed hydrogen/air combustion in a micro planar combustor with parallel separating plates. *International Journal of Hydrogen Energy* 40(5), 2396-403.
- Tang, A., Y. Xu, J. Pan, W. Yang, D. Jiang and Q. Lu (2015b). Combustion characteristics and performance evaluation of premixed methane/air with hydrogen addition in a micro-planar combustor. *Chemical engineering science* 131,235-42.
- Turns, S. R. (2002). *An Introduction to combustion: Concepts and Applications*. Second Edi. Mc Graw Hill; 200AD.
- Wan, J., A. Fan, H. Yao and W. (2015) Flame-anchoring mechanisms of a micro cavity-combustor for premixed H₂/air flame. *Chemical Engineering Journal* 275, 17-26.
- Wan, J., A. Fan, K. Maruta, H. Yao and W. Liu (2012) Experimental and numerical investigation on combustion characteristics of premixed hydrogen/air flame in a micro-combustor with a bluff body. *International Journal of Hydrogen Energy* 37(24), 19190-7.
- Wenming, Y., J. Dongyue, C. K. Kenny, Z. Dan and P. Jianfeng (2015). Combustion process and entropy generation in a novel microcombustor with a block insert. *Chemical Engineering Journal* 274, 231-7.
- Williams, F. A. (1965) *Combustion theory: the fundamental theory of chemical reacting flow systems*.
- Xue, H., W. Yang, S. K. Chou, C. Shu and Z. Li (2005) Microthermophotovoltaics power system for portable MEMS devices. *Microscale thermophysical engineering* 9(1), 85-97.
- Yang, W. M., K. J. Chua, J. F. Pan and D. Y. Jiang (2014) An H. Development of micro-thermophotovoltaic power generator with heat recuperation. *Energy conversion and management* 78, 81-7.
- Yang, W. M., S. K. Chou, C. Shu, Z. W. Li and H. Xue (2002) Development of microthermophotovoltaic system. *Applied physics letters* 81(27), 5255-7.
- Yang, W. M., S. K. Chou, C. Shu, Z. W. Li and H. Xue (2007) Experimental study of micro-thermophotovoltaic systems with different combustor configurations. *Energy conversion and management* 48(4), 1238-44.
- Zuo, W., E. Jiaqiang, Q. Peng, X. Zhao, Z. Zhang (2017). Numerical investigations on thermal performance of a micro-cylindrical combustor with gradually reduced wall thickness. *Applied Thermal Engineering* 113,1011-20.